INORGANIC CHEMISTRY
FRONTIERS

RESEARCH ARTICLE

View Article Online
View Journal | View Issue

Cite this: *Inorg. Chem. Front.*, 2023, **10**, 1887

In situ pyrazolylborate ligand synthesis and coordination behaviours in aluminum oxo clusters†

Jian-Bing Chen,[a,b] San-Tai Wang,[a,c] Si-Hao Shen,[a,c] Ying-Hua Yu,[a,c] Wei-Hui Fang *[a] and Jian Zhang *[a]

Received 9th January 2023,
Accepted 9th February 2023

DOI: 10.1039/d3qi00057e

rsc.li/frontiers-inorganic

Herein we describe the discovery of the *in situ* synthesis of pyrazolylborate ligands and their coordination behaviours towards Al(III) ions. The *in situ* synthesis of pyrazolylborate is facile, inexpensive and the resistant ligands of varying steric demand are readily accessible. The occurrence of such an *in situ* synthesis is related to the presence of $Al(^{i}OPr)_3$ Lewis acids. Compared with the classical N,N′,N″ tridentate *cis*-chelating pyrazolylborate scorpionate ligands, the *in situ* version herein having two pyrazolyls located at the opposite sides of the phenylboronic acid plane forms N,O,N′ *trans*-chelating ligands. We then studied the advantageous and coordination behaviours of the *trans*-coordinating ligands with Al(III) ions. The substituents on pyrazolyl and benzoyl rings have an important effect on the size of molecular clusters. The structures obtained by changing the functional groups (*e.g.* 3-F, 4-F, and 3-Cl) on the benzene ring are all dimeric molecules as shown in the **AlOC-126** series. When changing both the substituents on pyrazole and benzene rings, higher nuclearity tetrahedral **AlOC-127** and hexanuclear **AlOC-128** were isolated. The *in situ* formation of the ligand represents a potential new direction for the development of *trans*-chelating scorpionate analogues.

Introduction

Boron is a metalloid element with unique properties, and its unique electron-deficient structure has potential applications in assembling functionalized ligands.[1–3] These include phenylboronic acid derivatives, boronenes, diborenes, diborynes, and boron-containing heterocycles with potential applications in the biomedical field and light-harvesting fluorescent dyes.[4,5] Boron-centered ligands form metal complexes through multiple binding modes, which endow the resulting complexes with unique and unexpected properties. In inorganic chemistry, the planar $[BO_3]^{3-}$ anionic group is the most suitable basic structural unit of nonlinear optical crystals for ultraviolet and deep-UV light generation.[6] On the organic aspect, the first covalent organic frameworks (COF-1) have been successfully synthesized by condensation reactions of phenyl diboronic acid and hexahydroxytriphenylene.[7] As common bridging ligands, pyrazole and its derivatives not only can be used as electron donors to covalently bond with the B center, but also have a wide range of applications in cluster science.[8–12]

As the oldest and most classic examples of scorpionate ligand systems, poly(pyrazol-1-yl)borates ("scorpionates") with the general formula $[R'R''B(^{R}pz)_2]$ were first reported by Trofimenko in 1967 during the early origin of the scorpion ligand class.[13,14] Such ligands are widely used in coordination chemistry, from bioinorganic chemistry, homogeneous catalysis to materials science, and their complexes with most metals or metalloids in the periodic table have been prepared.[15] In order to stabilize the metal complexes and influence the angle of coordination to the metal, "second-generation scorpionates" that have a substituent with large steric hindrance (*e.g.* Ph and ^{t}Bu) on the 3-position of the pyrazole ring have been developed and widely used.[16] "The third generation" of scorpion ligands have full F substitution on the benzene ring, and through comparison it has been found that there are great differences between the crystal packing and electrical properties of the complexes of perfluorinated and non-fluorinated species.[17] Then, to further expand the range of scorpion ligands, Wagner

[a]*State Key Laboratory of Structural Chemistry, Fujian Institute of Research on the Structure of Matter, Chinese Academy of Sciences, Fuzhou, Fujian 350002, P. R. China. E-mail: fwh@fjirsm.ac.cn, zhj@fjirsm.ac.cn*
[b]*School of Physical Science and Technology, ShanghaiTech University, Shanghai 201210, P. R. China*
[c]*University of Chinese Academy of Sciences, Chinese Academy of Sciences, Beijing 100049, P. R. China*

†Electronic supplementary information (ESI) available: Full experimental details, supplementary figures and tables, PXRD, Raman spectroscopy, X-ray spectroscopy (EDS), and TGA spectra. CCDC 2234654–2234659. For ESI and crystallographic data in CIF or other electronic format see DOI: https://doi.org/10.1039/d3qi00057e

and coworkers developed "the fourth generation" of scorpion ligands, controlled their space requirements, and designed more flexible (N,N,N) and (N,O,N) types in the conformation of two mixed donors, making the structure more flexible and stable.[18] The above-mentioned scorpion ligands not only are rich in coordination sites, but also have adjustable steric hindrance, which has potential application value in synthetic structures.[15] However, from the development to the chelation of metals, the reaction process of this kind of ligand is complex and lengthy, and it is easy to form a single configuration, such as the [ML_2] mode of forming a double ligand to chelate a single metal.[19]

Based on the above considerations and our team's research focus on boronimidazole (BIF) ligands and our recently developed pyrazole-thermal synthesis,[20–22] we are hence interested in the exploration of scorpionate ligands. In addition to chelating monometallic compounds, such ligands should also be applicable in the cluster field. Considering the current structural type of scorpionates, we planned to design ligands with mixed sites for a wide range of metal ion chelation and cluster generation. By reacting phenylboronic acid, pyrazole and aluminum isopropanol, we found that phenylboronic acid reacts with pyrazole *in situ* to form tridentate scorpionates containing mixed N,O,N sites (Scheme 1). Although phenylboronic acid has been shown to be dehydrated and condensed *in situ* in solvothermal synthesis,[23,24] the *in situ* formation of such scorpionates is unprecedented. This *in situ* reaction is ubiquitous and can occur regardless of whether the substituents change on pyrazole or phenylboronic acid (Scheme 1). They present a mixed N, O, N donor set to the metal ion and the angle between the two pyrazolyls is sufficiently large for the metal binding. Therefore, the *in situ* ligands play an important role in inducing the aggregation of cluster compounds. Compared with the reported monomers and dimers bridged by classically prepared scorpionates,[14,25–27] we successfully isolated a series of aluminum oxo clusters (AlOCs) *via* the *in situ* generation method. These ligands chelate two Al ions at the same time, acting as "edge" ligands and constructing dimeric, tetrahedral and belt-like hexanuclear clusters (Fig. S1†). The formation of these compounds includes typical reactions involving both covalent bonds and coordinate bonds.

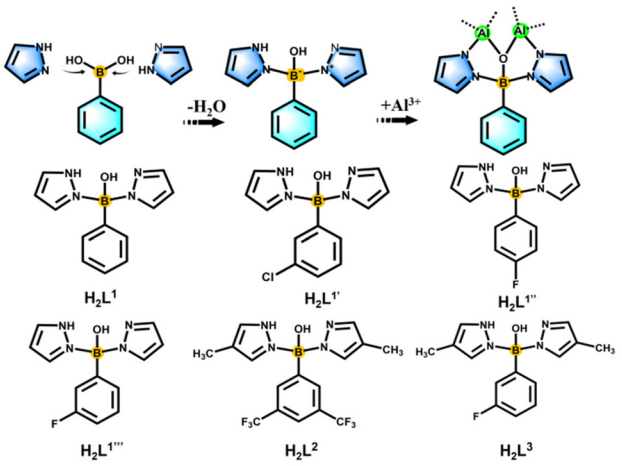

Scheme 1 Reaction herein involving both *in situ* generated covalent bond and coordinate bond with Al^{3+}. Although these ligands cannot be isolated, we have listed them in detail in order to give a clearer picture of the ligands on each compound and the universality of the *in situ* reaction.

Results and discussion

In our previous work, pyrazole-thermal synthesis is an effective way to prepare aluminum oxo clusters (AlOCs).[21,22] In this system, low melting point pyrazole (melting point: 66–70 °C) and 4-methyl-1*H*-pyrazole with a lower melting point (13 °C) are used not only as a reaction medium but also as the source of the *in situ* generation of scorpionates and the auxiliary ligand. Acetonitrile was selected as the auxiliary solvent to help promote dissolution and crystallization. Aluminum isopropoxide was added and it not only served as the source of metal Al ions but also promoted the dehydration reaction of phenylboronic acid.[28] Treatment of aluminum isopropoxide with phenylboronic acid and pyrazole in acetonitrile at 100 °C gives block colourless crystals of compound [$Al_2(L^1)_2(HL^1)_2$·MeCN] (**AlOC-126**, L^1 = PhB(μ-O)$(pz)_2$) (Fig. 1a and Scheme 1). The analogous reaction by changing different functional groups on the benzene ring resulted in the formation of the corresponding compounds [$Al_2(L^{1'})_2(HL^{1'})_2$·MeCN] (**AlOC-126-1**, $L^{1'}$ = (3-F-PhB(μ-O)$(pz)_2$), [$Al_2(L^{1''})_2(HL^{1''})_2$] (**AlOC-126-2**, $L^{1''}$ = (4-F-PhB(μ-O)$(pz)_2$) and [$Al_2(L^{1'''})_2(HL^{1'''})_2$] (**AlOC-126-3**, $L^{1'''}$ = (3-Cl-Ph(B(μ-O)$(pz)_2$) (Fig. 1a and Scheme 1). When different functional groups of phenylboronic acid are introduced through 4-methyl-1*H*-pyrazoles as the solvent, we obtained higher nuclearity (Fig. 1b, S3 and S4†). [$Al_4(L^2)_4(\mu_3\text{-O})(pz\text{-}CH_3)_3$)·MeCN] (**AlOC-127**, L^2 = (3,5-bis-CF_3-PhB(μ-O)$(pz\text{-}CH_3)_2$) is obtained when 3,5-bis(trifluoromethyl)phenylboronic acid is introduced and [$Al_6(L^3)_6(\mu_3\text{-O})_2(pz\text{-}CH_3)_2$] (**AlOC-128**, L^3 = (3-F-PhB(μ-O)$(pz\text{-}CH_3)_2$) is obtained when 3-F phenylboronic acid is introduced. Attempts to isolate related pyrazolylborate ligands using larger hindered ligands such as naphthalene boric acid and 3,5-dimethylpyrazole failed due to their differences in steric hindrance, melting point, and solubility.

All the compounds under investigation were structurally characterised by X-ray crystallography (Table S1†). Since the **AlOC-126** series of compounds are isostructural compounds that possess the same molecular cluster structures, only the structure of **AlOC-126** is discussed in detail here (Fig. 2 and S2†). As shown in Fig. 2a and b, compound **AlOC-126** is a butterfly-shaped dimer molecule. Four pyrazolylborate ligands on this molecule exhibit two coordination patterns, including μ_2–η^1:η^2:η^1 bridges and a terminal coordination mode (Fig. 2c). Two tridentate ligands participate in binding with two Al^{3+} through three sites (N, O, N), while the other two hang on them to complete the octahedral coordination environment of Al ions. Bond valence sum (BVS) calculations (Table S2†) and charge balance indicate that the two terminal ligands are par-

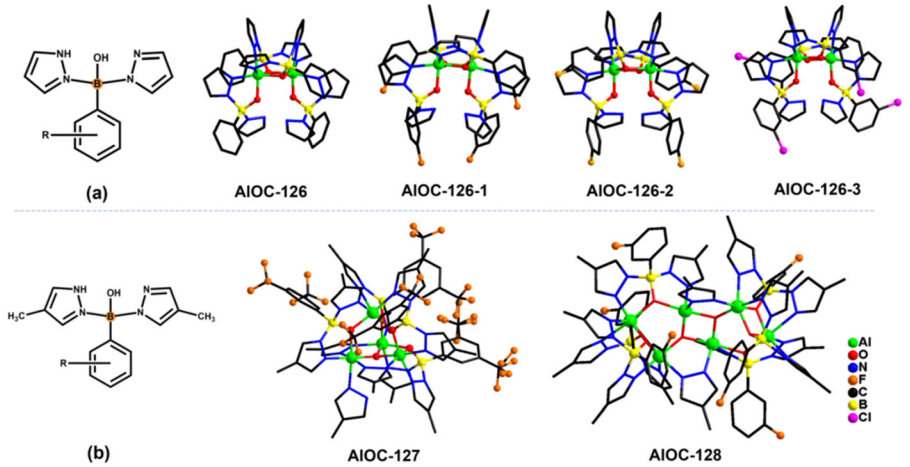

Fig. 1 A display of all compounds isolated herein showing the association of structure type and ligand regulation. (a) The alternation of functional groups on the benzene ring results in the **AlOC-126** series. (b) The change on both the benzene ring and pyrazole brings the nuclearity increment, see compounds **AlOC-127** and **AlOC-128**.

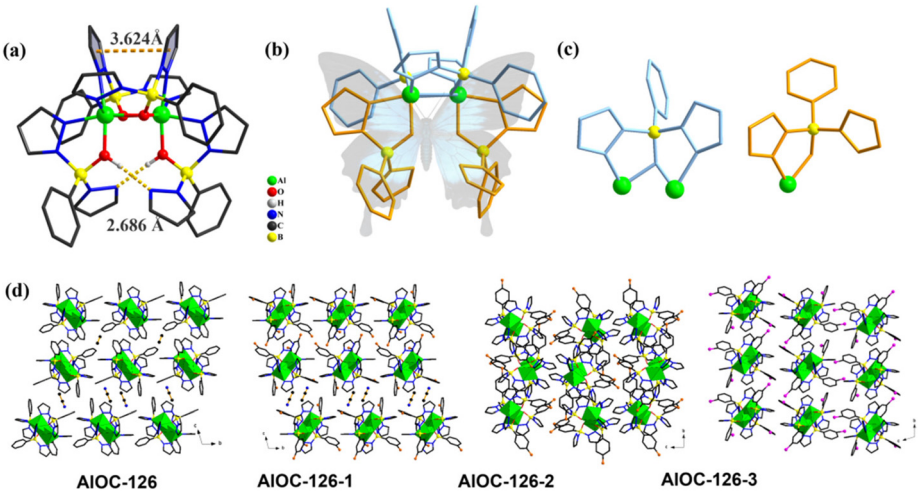

Fig. 2 The molecular structures of the dimers of **AlOC-126** series. (a) Molecular structures of **AlOC-126** and coordination environment of Al(III). (b) Simplified structure of **AlOC-126**. (c) Coordination mode of [Ph(pz)B(μ-O)(pz)]. (d) Lattice arrangements of **AlOC-126** series (color code: Al green; B yellow; O red; N blue; C black).

tially deprotonated and the position of the proton was found to be on the B atoms. It is worth noting that there are abundant weak interactions within the molecule, containing hydrogen bonds (O–H···N, 2.6 Å) and π···π interactions (3.624 Å) (Fig. 2a). Therefore, such a molecular configuration is very stable, and isomorphic compounds can be obtained by changing the functional groups on the benzene ring (Fig. 1a). But the presence of these functional groups affects the intermolecular interactions, lattice arrangements and supramolecular structures (Fig. 2d).

The X-ray crystal structure analysis reveals that compound **AlOC-127** is a tetranuclear compound crystallizing in the triclinic space group $P\bar{1}$ (Fig. 3a). The four Al^{3+} atoms of **AlOC-127** are at the apex of a tetrahedron with the base fused by a μ_3-O. Four of the six edges of the tetrahedron were bridged by four tridentate L^2 pyrazolylborates (Fig. S3†). And the other two edges were linked by two pyrazoles (Fig. 3b). The octahedral coordination environment of the Al ion between these two 4-methylpyrazoles was further completed by a third terminal 4-methylpyrazole. We can see a significant difference in the four L^2 ligands. It is worth noting that although these ligands share the same chelation pattern, the spatial arrangement of the ligands is not the same. The benzene and pyrazole on the ligand exhibit two types of torsions and arrangements (Fig. 3c). One type has a benzene ring pointing to the paper surface (defined as a vertical pattern), and the other has a benzene ring approximately parallel to the paper surface (defined as a parallel pattern). The three ligands located on the waist of the tetrahedron are arranged in the vertical pattern, while the L^2 on the base adopts the parallel arrange-

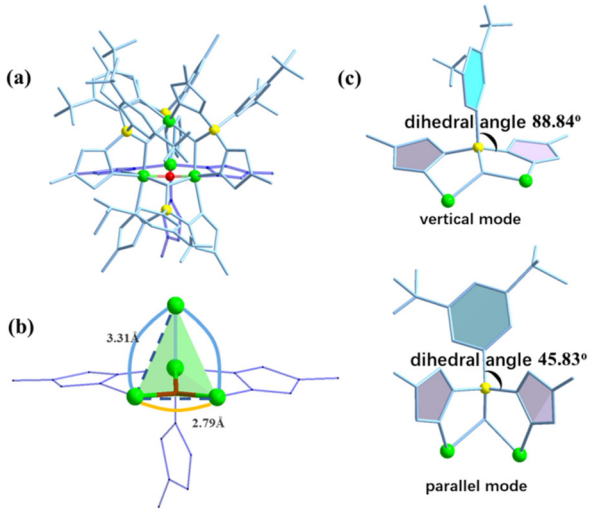

Fig. 3 (a) Molecular structures of **AlOC-127** and the coordination environment of Al(III); (b) core structure of **AlOC-127**. The vertical mode and parallel mode of L^2 ligands are presented as blue and yellow lines for clarity. (c) The presentation of the vertical mode and parallel mode of L^2 ligands (color code: Al, green; B, yellow; O, red; N, blue; C, black).

ment. Correspondingly, the Al···Al distances also have a certain difference, where the Al···Al distances of 3.31 Å, 3.35 Å and 3.37 Å are bridged by the vertical pattern, and the Al···Al distance of 2.79 Å is significantly smaller and linked by the parallel pattern. The reason for this could be the overall combination of a free-rotating benzene ring, steric hindrance, a flexible B tetrahedral center and an Al octahedral center.

Compound **AlOC-128** possesses a ribbon-like hexanuclear structure (Fig. 4a). Its core structure is shown in Fig. 4b. The 4 aluminum atoms in the center are connected by two oxygen bridges and 4-methylpyrazole. The aluminum ions at both ends are further connected to it by 6 L^3 ligands (Fig. S4†). Within the six L^3 ligands, four are in parallel mode and two are in vertical mode. The parallel : vertical mode ratio of 2 : 1 is significantly large than that of 1 : 3 in **AlOC-127**. This may be due to a change in the spatial arrangement of the ligand, depending on the type of structure, a cage-like or ribbon-like structure. We found obvious intramolecular π···π conjugation (3.318 Å) between 4-methylpyrazole in this structure (Fig. 4c). In addition, intermolecular hydrogen bonds are also observed. The lattice arrangements of **AlOC-126** to **AlOC-128** are shown in Fig. S5–S7.†

The phase purity and stability of these compounds were verified by powder X-ray diffraction (PXRD) analysis (Fig. S9–S14†). In infrared spectrum analysis (Fig. S15–S17†), the infrared spectrum of **AlOC-126** shows an obvious absorption band corresponding to the unprotonated –OH unique to **AlOC-126** at about 1400 cm^{-1} (δ_{OH}). **AlOC-127** and **AlOC-128** also showed the methyl groups and the fluorination groups on benzene rings at about 2933 cm^{-1} (ν_{C-H}) and 1107 cm^{-1} (ν_{C-F}). The presence of elements (Al, C, N, O and F) in **AlOC-126** to **AlOC-128** has been validated using EDS spectra (Fig. S18–S20†). In addition, with the increase of the number of F functional groups introduced into the benzene ring, the relative peak area of the F element also increased, and the relative peak area of the F element reached the maximum when 3,5-bis (trifluoromethyl)phenylboric acid was introduced (Fig. S19†). The solid-state UV-vis absorption spectra of **AlOC-126** to **AlOC-128** are obtained from the data of the diffuse-reflectance spectra (Fig. 5). They show no absorption above 300 nm, which is in accordance with their colorless crystals. The crystal morphology of **AlOC-126** is a colorless flat-angled rhombic cube, the crystal morphology of **AlOC-127** is a colorless parallele-

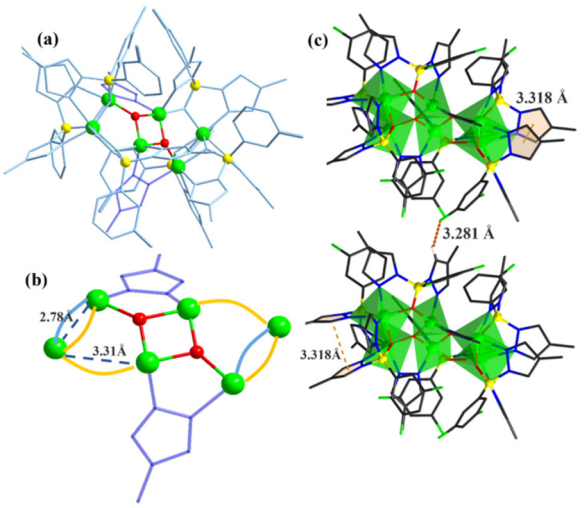

Fig. 4 (a) Molecular structures of **AlOC-128** and the coordination environment of Al(III) and (b) the core structure of **AlOC-128**. The vertical mode and parallel mode of L^2 ligands are presented as blue and yellow lines for clarity. (c) The intramolecular and intermolecular interactions (color code: Al, green; B, yellow; O, red; N, blue; C, black).

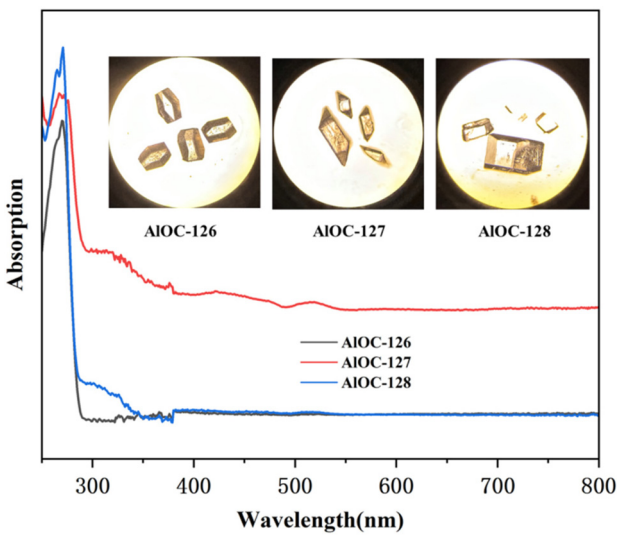

Fig. 5 Solid-state UV–vis absorption spectra. The inset shows their crystal pictures observed under a microscope.

piped, and the crystal morphology of **AlOC-128** is a colorless brick (Fig. 5). According to the Kubelka–Munk function, the optical band gap of **AlOC-126** to **AlOC-128** is about 4.2–4.4 eV (Fig. S21–S23†). The thermal stability of **AlOC-126** to **AlOC-128** was characterized by thermogravimetric analysis (TGA) (Fig. S24†).

The *in situ* generated pyrazolylborates possess abundant aromatic five-membered and six-membered rings. In addition, their intramolecular π···π conjugation also encourages us to investigate their third-order NLO properties. The convenient *Z*-scan technique is widely used to measure the nonlinear absorption coefficient of materials. The experimental results of open aperture (OA) *Z*-scan measurement at a pulse energy of 4 μJ are recorded using a picosecond laser with a wavelength of 532 nm and a repetition rate of 10 Hz. In order to compare the NLO effect and adjust the sample concentration, a similar linear transmittance of 65% was obtained at 532 nm in 1 mm thick cells. The NLO and optical limit (OL) properties of the samples are analyzed, and the results are shown in Fig. 6a. All OA *Z*-scan curves show a decrease in transmittance at the focal point of the laser beam where the input flux is maximum. Under the same test conditions, the minimum normalized transmittance (T_{min}) of the measured samples at the focal point ($Z = 0$) showed the following order: **AlOC-128** > **AlOC-127** > **AlOC-126** (Fig. 6a). The three compounds exhibit remarkable nonlinear optical response and reverse saturated absorption (RSA). We believe that the clear RSA response of these crystalline materials is mainly attributable to the conjugation of aromatic rings between benzene rings and pyrazoles, pyrazoles and pyrazoles on two adjacent ligands. Comparison of the nonlinear optical parameter values among the three samples is provided in Table S3.† In order to quantitatively evaluate the NLO response, the nonlinear absorption coefficients (β) of **AlOC-126**, **AlOC-127**, and **AlOC-128** were calculated by fitting nonlinear correlation equations, which were 0.41, 0.58, and 0.87 cm GW^{-1}, respectively, and are comparable to those of gold nanoparticle-doped GeO_2–Bi_2O_3 glasses, phthalocyanine compounds, and some traditional crystal materials.[29–32] The curve shows the change of the normalized transmittance and the input flux. As the input luminous flux increases, the transmittances of the three samples decrease to 72%, 65% and 52%, respectively (Fig. 6a and b).

Further structural analysis revealed that the OL effect is not only related to the generally reported π···π interaction, but also related to the hydrogen bond interaction, atomic polarizability, and molecular band gap. Although both **AlOC-126** and **AlOC-127** have three pairs of π···π interactions, the three pairs of π···π interactions of **AlOC-127** are stronger than those of **AlOC-126**, and **AlOC-128** has the most π···π interaction pairs, and its corresponding RSA response is also the largest (Fig. 6c). In our study, the band gaps of the three sample compounds are all around 4.2 eV, which is higher than the single-photon energy (2.33 eV) at 532 nm, which is favorable for two-photon absorption. In addition, **AlOC-127** and **AlOC-128** also

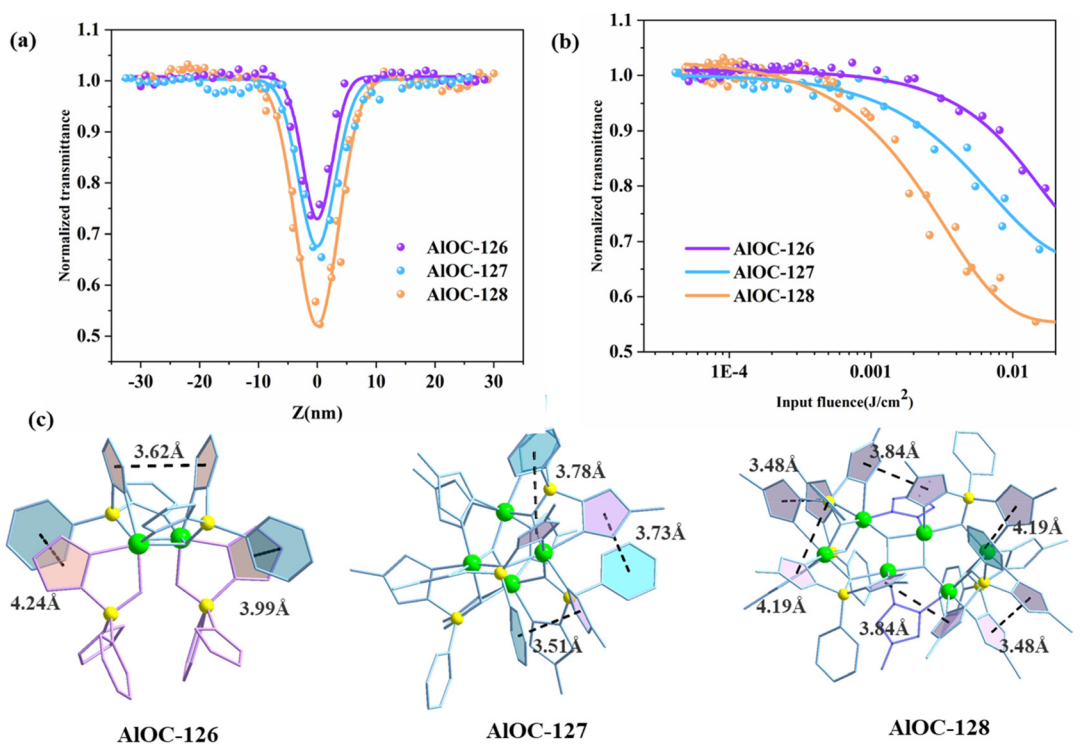

Fig. 6 (a) OA *Z*-scan curves and (b) OL curves of the samples at picosecond laser excitation (input energy: 4 μJ). The linear transmittance of the samples was adjusted to be 65%. Colored scattered balls indicate experimental data with the solid line representing the curve of best fit. (c) π···π interactions between adjacent L in **AlOC-126**, **AlOC-127**, and **AlOC-128**. Color code: Al, green; B, yellow.

show abundant hydrogen bond interactions (C–H···F) (Fig. S8†). Fluorine is the most electronegative element, and the push–pull electron effect has a positive effect on the electron transport density and polarizability, thereby promoting non-linear absorption.[33] Therefore, in general, **AlOC-127** and **AlOC-128** with F substituents introduced on the benzene ring have better nonlinear absorption.

Conclusions

In summary, we developed a facile synthetic strategy for the isolation of pyrazolylborate ligands. The *in situ* generation method provides a very stable platform for the development of *trans*-chelating scorpionate analogues. Such kinds of ligands exhibit great adaptive coordination behaviors and have great potential in cluster science. The metal ions could be extended to a broad range of other Lewis acid metal ions such as titanium ions. Related work on exploiting the coordination behavior with other metal ions is underway.

Data availability

The datasets supporting this article have been uploaded as part of the ESI.† CCDC reference numbers 2234657 (**AlOC-126**), 2234654 (**AlOC-126-1**), 2234655 (**AlOC-126-2**), 2234658 (**AlOC-126-3**), 2234659 (**AlOC-127**) and 2234656 (**AlOC-128**) contain the X-ray crystallographic data.†

Author contributions

All authors contributed extensively to the work presented in this paper. J. Zhang and W.-H. Fang conceived the research project. J.-B. Chen performed the synthesis, characterization and third-order NLO property analysis. S.-H. Shen assisted with the data collection and analysis. S.-T. Wang assisted with the refinement of crystal data. Y.-H. Yu assisted with structural analysis. W.-H. Fang and J.-B. Chen wrote the manuscript and ESI† with input from the other authors.

Conflicts of interest

There are no conflicts to declare.

Acknowledgements

The research reported in this publication was supported by the National Natural Science Foundation of China (92061104, 21973096), Natural Science Foundation of Fujian Province (2021J06035) and Youth Innovation Promotion Association of Chinese Academy of Sciences (Y2018081).

References

1 M. M. Díaz-Requejo, M. A. Mairena, T. R. Belderrain, M. C. Nicasio, S. Trofimenko and P. J. Pérez, A family of highly active copper(I)–homoscorpionate catalysts for the alkyne cyclopropenation reaction, *Chem. Commun.*, 2001, 1804–1805.
2 J. A. López, K. Mereiter, M. Paneque, M. L. Poveda, O. Serrano, S. Trofimenko and E. Carmona, Unusual fragmentation of CH_2Cl_2 by an Ir(III) centre bonded to a doubly metalated Tp^{Ms} Ligand (Tp^{Ms} = hydrotris(3-mesitylpyrazol-1-yl)borate), *Chem. Commun.*, 2006, 3921–3923.
3 L. Nurdin, W. E. Piers, J.-B. Lin and B. S. Gelfand, Synthesis, Characterization, and Reactivity of Neutral Octahedral Alkyl-Cobalt(III) Complexes Bearing a Dianionic Pentadentate Ligand, *Organometallics*, 2020, **39**, 2269–2277.
4 J. T. Goettel and H. Braunschweig, Recent advances in boron-centered ligands and their transition metal complexes, *Coord. Chem. Rev.*, 2019, **380**, 184–200.
5 M. Henkelmann, A. Omlor, M. Bolte, V. Schunemann, H. W. Lerner, J. Noga, P. Hrobarik and M. Wagner, A free boratriptycene-type Lewis superacid, *Chem. Sci.*, 2022, **13**, 1608–1617.
6 C. T. Chen, B. C. Wu, A. D. Jiang and G. M. You, a new-type ultraviolet SHG crystal - Beta-BaB_2O_4, *Sci. Sin., Ser. B*, 1985, **28**, 235–243.
7 A. P. Cote, A. I. Benin, N. W. Ockwig, M. O'Keeffe, A. J. Matzger and O. M. Yaghi, Porous, Crystalline, Covalent Organic Frameworks, *Science*, 2005, **310**, 1166–1170.
8 Y.-K. Deng, H.-F. Su, J.-H. Xu, W.-G. Wang, M. Kurmoo, S.-C. Lin, Y.-Z. Tan, J. Jia, D. Sun and L.-S. Zheng, Hierarchical Assembly of a $\{Mn^{II}_{15}Mn^{III}_{4}\}$ Brucite Disc: Step-by-Step Formation and Ferrimagnetism, *J. Am. Chem. Soc.*, 2016, **138**, 1328–1334.
9 L.-Y. Guo, H.-F. Su, M. Kurmoo, C.-H. Tung, D. Sun and L.-S. Zheng, Core–Shell $\{Mn_7\subset(Mn,Cd)_{12}\}$ Assembled from Core $\{Mn_7\}$ Disc, *J. Am. Chem. Soc.*, 2017, **139**, 14033–14036.
10 B.-Q. Ji, H.-F. Su, M. Jagodič, Z. Jagličić, M. Kurmoo, X.-P. Wang, C.-H. Tung, Z.-Z. Cao and D. Sun, Self-Organization into Preferred Sites by Mg^{II}, Mn^{II}, and Mn^{III} in Brucite-Structured M_{19} Cluster, *Inorg. Chem.*, 2019, **58**, 3800–3806.
11 V. M. Leovac, R. Petković, A. Kovács, G. Pokol and K. M. Szécsényi, Reactions of divalent transition metal halides with 3,5-dimethyl-1-(hydroxymethyl)-pyrazole, *J. Therm. Anal. Calorim.*, 2007, **89**, 267–275.
12 W. Muhammad, J. Ni, Z. Jagličić, P. Cui, L. Gao and D. Sun, Synthesis, structure and magnetic properties of a decanuclear Fe(III)/oxo cluster, *Chin. Chem. Lett.*, 2020, **31**, 2503–2506.
13 S. Trofimenko, Scorpionates: genesis, milestones, prognosis, *Polyhedron*, 2004, **23**, 197–203.
14 S. Trofimenko, Boron-pyrazole chemistry. IV. Carbon- and boron-substituted poly[(1-pyrazolyl) borates], *J. Am. Chem. Soc.*, 1967, **89**, 6288–6294.
15 S. Bieller, M. Bolte, H. W. Lerner and M. Wagner, Modular approach to tridentate N,O,N′ ligands using pyrazolylborate chemistry, *Chem. – Eur. J.*, 2006, **12**, 4735–4742.

16 S. Trofimenko, J. C. Calabrese and J. S. Thompson, Novel polypyrazolylborate ligands: coordination control through 3-substituents of the pyrazole ring, *Inorg. Chem.*, 1987, **26**, 1507–1514.
17 P. J. Desrochers, A. J. Pearce, T. R. Rogers and J. S. Rodman, Rapid Synthesis of a Functional Resin–Supported Scorpionate and Its Copper(I, II), Rhodium(I), and Chromium(III) Complexes, *Eur. J. Inorg. Chem.*, 2016, 2465–2473.
18 E. V. Mutseneck, S. Bieller, M. Bolte, H. W. Lerner and M. Wagner, Fourth generation scorpionates: coordination behavior of a new class of conformationally flexible mixed-donor (pyrazol-1-yl)borates, *Inorg. Chem.*, 2010, **49**, 3540–3552.
19 E. V. Mutseneck, C. Reus, F. Schödel, M. Bolte, H.-W. Lerner and M. Wagner, Reactions of $[Cp^*RuCl]_4$ and $[(p\text{-cymene})RuCl_2]_2$ with the Tridentate Ligand $[Ph(pz)B(\mu\text{-}O)(\mu\text{-}pz)B(pz)Ph]^-$, *Organometallics*, 2010, **29**, 966–975.
20 J. Zhang, T. Wu, C. Zhou, S. Chen, P. Feng and X. Bu, Zeolitic boron imidazolate frameworks, *Angew. Chem., Int. Ed.*, 2009, **48**, 2542–2545.
21 X. Fan, H. Fu, M. Y. Gao, L. Zhang and J. Zhang, One-Pot and Postsynthetic Phenol-Thermal Synthesis toward Highly Stable Titanium-Oxo Clusters, *Inorg. Chem.*, 2019, **58**, 13353–13359.
22 S. Yao, W. H. Fang, Y. Sun, S. T. Wang and J. Zhang, Mesoporous Assembly of Aluminum Molecular Rings for Iodine Capture, *J. Am. Chem. Soc.*, 2021, **143**, 2325–2330.
23 X. J. Kong, T. He, Y. Z. Zhang, X. Q. Wu, S. N. Wang, M. M. Xu, G. R. Si and J. R. Li, Constructing new metal-organic frameworks with complicated ligands from "One-Pot" in situ reactions, *Chem. Sci.*, 2019, **10**, 3949–3955.
24 X.-Z. Zhang, W.-H. Fang and X.-F. Wang, An *in situ* esterification reaction in amino-alcohols coordinated aluminum oxo clusters, *Inorg. Chem. Commun.*, 2021, **128**, 108608.
25 M. Bortoluzzi, V. Ferraro and F. Sartor, Photoluminescence of Homoleptic Lanthanide Complexes With Tris(benzotriazol-1-yl)borate, *J. Fluoresc.*, 2021, **31**, 1433–1443.
26 M. Narwane, D. P. Dorairaj, Y. L. Chang, R. Karvembu, Y. H. Huang, H. W. Chang and S. C. N. Hsu, Tris-(2-pyridyl)-pyrazolyl Borate Zinc(II) Complexes: Synthesis, DNA/Protein Binding and In Vitro Cytotoxicity Studies, *Molecules*, 2021, **26**, 7341.
27 G. Wang, A. Noonikara-Poyil, I. Fernandez and H. V. R. Dias, Iron pentacarbonyl ligands on silver scorpionates, *Chem. Commun.*, 2022, **58**, 3222–3225.
28 C. Chen and R. F. Jordan, Lewis Acid Catalyzed Synthesis of Poly(pyrazolyl)borate Ligands, *Organometallics*, 2010, **29**, 3679–3682.
29 Y. Chen, M. Hanack, Y. Araki and O. Ito, Axially modified gallium phthalocyanines and naphthalocyanines for optical limiting, *Chem. Soc. Rev.*, 2005, **34**, 517–529.
30 S. Perumbilavil, A. López-Ortega, G. K. Tiwari, J. Nogués, T. Endo and R. Philip, Enhanced Ultrafast Nonlinear Optical Response in Ferrite Core/Shell Nanostructures with Excellent Optical Limiting Performance, *Small*, 2018, **14**, 1701001.
31 D. Ramachari, L. Rama Moorthy and C. K. Jayasankar, Gain properties and concentration quenching of Er^{3+}-doped niobium oxyfluorosilicate glasses for photonic applications, *Opt. Mater.*, 2014, **36**, 823–828.
32 J.-L. Wang, M.-X. Yang, N.-F. Li, X.-M. Liu, J.-N. Li, Q.-D. Ping and Y. Xu, Two Ni-Substituted Trilacunary Keggin-Type Polyoxometalates: Syntheses, Crystal Structures, NLO Studies, and Magnetic Properties, *Inorg. Chem.*, 2021, **60**, 13748–13755.
33 F. Kong, T.-K. Jiang and J.-G. Mao, Role of fluorine on the structure and second-harmonic-generation property of inorganic selenites and tellurites, *Chem. Commun.*, 2021, **57**, 12575–12586.